AIAA SciTech Forum
6-10 January 2020, Orlando, FL
AIAA Scitech 2020 Forum

10.2514/6.2020-0011

Development of an Efficient Mach=0.80 Transonic Truss-Braced Wing Aircraft

Neal A. Harrison*, Michael D. Beyar†, Eric D. Dickey‡, Krishna Hoffman§
Boeing Research and Technology, Huntington Beach, CA, 92647, USA

Gregory M. Gatlin** and Sally A. Viken††
NASA Langley Research Center, Hampton, VA, 23681, USA

An update is presented regarding current status of work undertaken as a part of the Subsonic Ultra-Green Aircraft Research (SUGAR) Phase IV contract funded by the NASA Advanced Air Transport Technology (AATT) project. The work herein describes progress made in the current phase of study and highlights remaining challenges associated with further maturation of the Transonic Truss-Braced Wing (TTBW) concept.

In SUGAR Phase IV, the development of a TTBW vehicle designed for efficient cruise operation at Mach 0.80 has been undertaken, including the development of a high-lift system design suitable for this class of aircraft. The high and low-speed aerodynamic designs were validated by wind tunnel testing at the NASA Ames Unitary Plan Wind Tunnel (UPWT) and NASA Langley 14- by 22-Foot Subsonic Tunnel, respectively. These tests were used to assess the predicted design performance, and help identify any potential design challenges and requirements for future concept development. In addition, this effort has also addressed the aeroelastic behavior of the revised TTBW configuration, and identified areas of future focus in structural development.

I. Nomenclature

α	=	Vehicle angle of attack, degrees
AATT	=	Advanced Air Transport Technology
AAVP	=	Advanced Air Vehicles Program
ANTS	=	Automated Navier-Stokes Two-dimensional Setup
ARC	=	Ames Research Center (NASA)
C_D	=	Vehicle Drag coefficient
CFD	=	Computational Fluid Dynamics
C_L	=	Vehicle Lift coefficient
c_{lmax}	=	Airfoil sectional maximum lift coefficient
DL	=	Doublet Lattice
eta	=	Fraction of wing semispan
FCK	=	Fixed Camber Krueger
FEM	=	Finite Element Model
UPWT	=	Unitary Plan Wind Tunnel (NASA)
LaRC	=	Langley Research Center (NASA)
L/D	=	Vehicle Lift-to-Drag ratio
M	=	Mach number
MDM	=	Model Deformation Measurement
RANS	=	Reynolds-Average Navier Stokes
Re	=	Unit Reynolds number, per Foot
SUGAR	=	Subsonic Ultra Green Aircraft Research
TTBW	=	Transonic Truss-Braced Wing
TWT	=	Transonic Wind Tunnel
VCK	=	Variable Camber Krueger
x/c	=	Chordwise length as a fraction of local wing chord
y/c	=	Height as a fraction of local wing chord

* SUGAR Project Manager, Boeing Research & Technology - Aerosciences, Senior Member AIAA
† Aerodynamics Engineer, Boeing Research & Technology - Aerosciences, Member AIAA
‡ Aerodynamics Engineer, Boeing Research & Technology - Aerosciences
§ Structural Analysis Engineer, BR&T Advanced Structural Design
** Senior Research Engineer, Configuration Aerodynamics Branch, Mail Stop 267, AIAA Associate Fellow
†† Assistant Head, Configuration Aerodynamics Branch, Mail Stop 499, AIAA Associate Fellow

II. Introduction

The objective of the NASA Advanced Air Vehicles Program (AAVP) is to advance technologies that show significant potential for revolutionary improvements in aircraft efficiency, emissions, noise, and safety as compared to conventional cantilever-wing aircraft. Within this program, the Advanced Air Transport Technology (AATT) project matures fixed-wing commercial transport technologies that offer the greatest potential to meet these objectives. The AATT project's target metrics for dramatic reductions in noise, emissions, and fuel consumption as a function of near, mid, and far-term objectives are shown in Figure 1.

TECHNOLOGY BENEFITS	**TECHNOLOGY GENERATIONS** Technology Readiness Level = 5/6		
	Near-Term 2015-2025	**Mid-Term** 2025-2035	**Far-Term** 2035+
Noise (cum below Stage 4)	**22 – 32 dB**	**32 – 42 dB**	**42 – 52 dB**
LTO NOx Emissions (cum below CAEP 6)	**70 – 75%**	**80%**	**>80%**
Cruise NOx Emissions (rel. to 2005 best in class)	**65 – 70%**	**80%**	**>80%**
Aircraft Fuel/Energy Consumption (rel. to 2005 best in class)	**40 – 50%**	**50 – 60%**	**60 – 80%**

Figure 1. NASA Subsonic Transport System-Level Metrics/Goals (1)

In December 2016 Boeing was awarded the SUGAR Phase IV contract to continue to investigate the enabling potential of Transonic Truss-Braced Wing (TTBW) technology to help satisfy the NASA objectives. Summaries of the work completed in previous phases of the SUGAR program may be found in open literature (2-6). In SUGAR Phase IV, the goal was to investigate and adapt the TTBW concept to transonic Mach numbers more consistent with today's commercial transport aircraft. Specifically, the TTBW concept was updated to operate at a cruise Mach number of 0.80. This work began by updating the preliminary Mach 0.80 design completed during SUGAR Phase III, and then extended to a detailed aerodynamic design of the configuration at both high and low-speeds, including the development of a laminar-flow compatible high-lift system. Both the high and low-speed designs underwent aerodynamic validation in a series of wind tunnel tests. The high-speed (transonic) design was tested in the NASA Ames 11-Foot Unitary Plan Wind Tunnel (UPWT) located at Moffett Field, CA beginning in July 2019, while the low-speed design was tested in the NASA Langley Research Center's 14- by 22-Foot Subsonic Tunnel beginning in September 2019.

In addition to aerodynamic development, the updated concept's structure was investigated. Aero-structural optimization was performed to study the trades between strut structural weight and vehicle aerodynamic performance. This included studies to examine the effect of variation in the location of the jury strut and the impact of using different strut construction materials. A global Finite Element Model (FEM) was constructed and used for updated structural sizing and weight estimates based on the revised loads. This design was then assessed for its aeroelastic behavior and performance. In addition, several conceptual designs of key structural joints were investigated.

III. Design and Test of Mach 0.80 TTBW

This paper outlines the tasks and objectives undertaken as a part of the SUGAR Phase IV contract. The primary objectives funded under this study are:

1) Design a TTBW configuration that can operate efficiently at a cruise Mach = 0.80, and validate the high-speed aerodynamic performance in a transonic wind tunnel test.
2) Develop a high-lift system for the TTBW vehicle, and validate the aerodynamic performance in a low-speed wind tunnel test.
3) Develop and compare an advanced tube-and-wing configuration of equivalent technology level to meet the same mission requirements as the TTBW vision vehicle.
4) Identify remaining technical challenges associated with application of TTBW technology to modern commercial aircraft, and develop a roadmap for the continued systematic reduction in risk.

The period of performance for Phase IV extended from January 2017 to March 2020. The overall timeline of the SUGAR program, including previous phases of study and key test campaigns is shown in Figure 2.

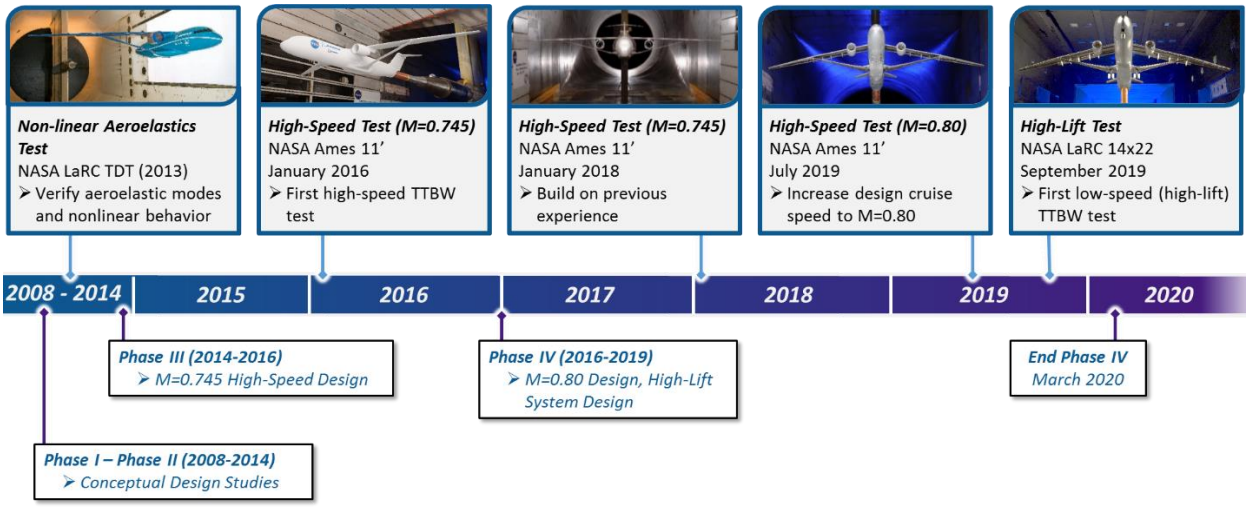

Figure 2. SUGAR Program timeline including key test campaigns

As shown above, the SUGAR program has now completed five major wind tunnel tests of the TTBW configuration. The demonstrations began with the non-linear aeroelastics test in the NASA Langley Research Center (LaRC) Transonic Dynamics Tunnel (TDT) in 2013, and was followed by three transonic performance wind tunnel tests at the NASA Ames Research Center (ARC) UPWT. Most recently, a low-speed test was conducted at the NASA LaRC 14- by 22-Foot Subsonic Tunnel to investigate the performance of the configuration's high-lift system. This test, completed in November 2019, represented the first time the TTBW's high-lift potential was measured in a high-fidelity wind tunnel test.

The following sections will describe in more detail the individual design and test efforts that comprised the Phase IV work.

A. Mach 0.80 TTBW Configuration Update

In SUGAR Phase III a preliminary Mach 0.80 design was created. The new geometry was based on a modification of the Phase III Mach=0.745 vehicle, with changes to wing sweep and airfoil thickness, as well as a rebalancing of the aircraft center of gravity realized by a shift in the wing root and landing gear locations. The wing and strut structural tie-in locations and wing planform were frozen for the study. Spanwise location of the wing-strut interface was maintained at ~58% span.

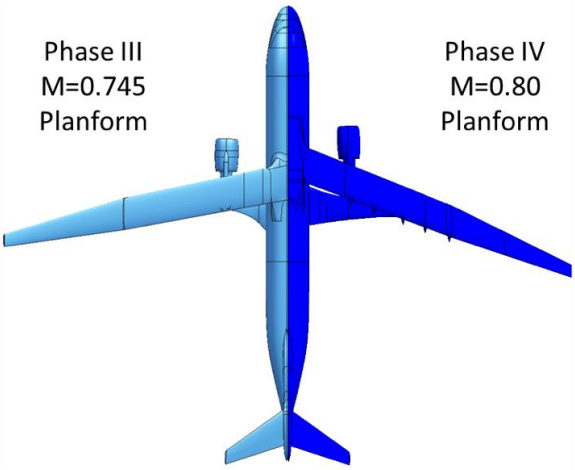

Figure 3. Comparison of the M=0.745 Phase III Planform to the Final M=0.80 Phase IV Planform

As shown in Figure 3, the most notable difference between the Phase III and IV designs was an 'unstacking' of the wing and inboard strut. By shifting the wing root forward the inboard strut no longer laid directly underneath the wing. As a result the aerodynamic interaction between these surfaces was (locally) reduced. The changes to the configuration layout were also found to have several additional positive effects, including:

1) *Reduced compressibility drag* – the unstacked geometry has a naturally improved vehicle cross-sectional area distribution as compared to the Phase III design.
2) *Protection of the inboard strut during high-lift operations* – by placing the inboard strut aft of the inboard wing-body attachment it is partially protected from large variations in flow onset angle since the wing acts like a flow-straightener. As a result, the inboard strut is less likely to separate during high-lift operations. This protection may preclude the necessity of leading-edge protection on the strut.
3) *Increased structural strength of the wing-strut system* – the in-plane strength of the wing-strut system is increased by the larger streamwise separation of the wing-body and strut-body attachment locations.

Following the definition of the updated M=0.80 aircraft configuration, a detailed high-speed design cycle was conducted.

B. High-Speed Design

The SUGAR Phase III design effort proved that a TTBW could operate efficiently at transonic cruise Mach numbers, and outlined the primary design strategies for achieving this goal [5]. However, since the M=0.80 vehicle configuration had been modified from its M=0.745 parent it was important to revisit the vehicle's aerodynamic design strategy. This allowed the designers to examine if the configuration changes provided new limitations or opportunities in its design beyond the lessons learned in Phase III.

The most significant of these considerations was to determine if changes to the inboard wing-strut proximity could affect the amount of lift that could efficiently be carried by the strut during cruise operations. In Phase III the location of the strut directly underneath the wing precluded it from carrying a substantial amount of load – any significant amount of lift generated on the strut would have the opposite effect on the wing. Thus, the staggering of the Phase IV wing and strut (root) thereby created the potential for the strut to contribute more significantly to the aerodynamic performance of the vehicle. This meant considering the strut as a primary lifting surface, rather than a structural element with a necessary, but manageable, contribution to vehicle parasitic drag. At the onset of the M=0.80 high-speed aerodynamic design the system-level implications of this strategy were unknown.

To execute this strategy, when designers began the M=0.80 aerodynamic design the wing and strut were by necessity designed together, with a view towards their total contribution to vehicle spanload. Preliminary M=0.80 designs therefore sought to significantly increase the amount of strut lift as compared to the Phase III designs. Figure 4 shows a comparison of the wing-strut spanloads between the Phase III design and an intermediate stage of the Phase IV design. The Phase IV strut loading demonstrates a significantly larger contribution to vehicle lift than the Phase III vehicle. As a consequence, the inboard wing loading is significantly reduced. To determine the final division of lift between the wing and strut designers relied on aerodynamic and multi-disciplinary design optimization methods.

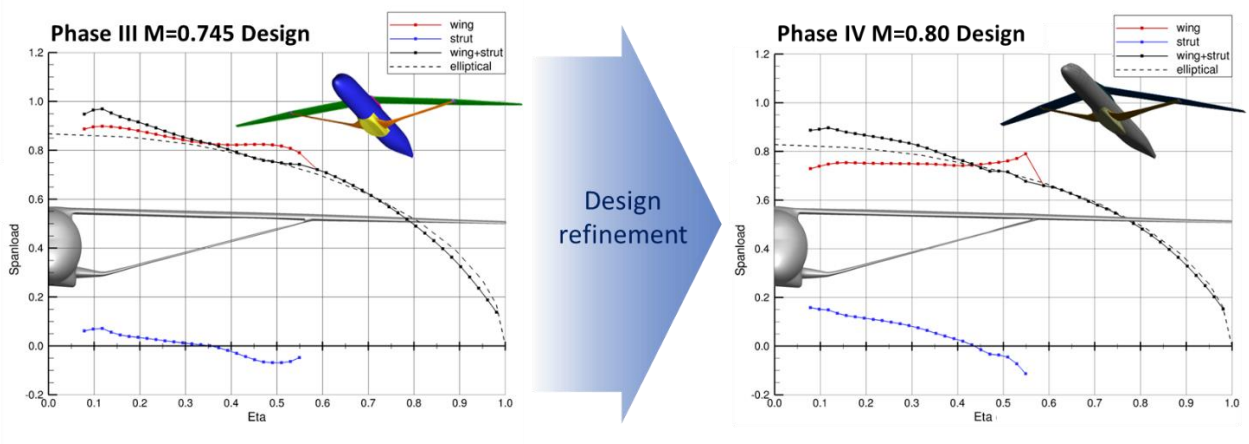

Figure 4. Design refinement of vehicle spanload (M=0.745 design vs. M=0.80 design)

The wing and strut are significantly coupled aerodynamically and structurally. The optimum design was therefore considered at the system-level, rather than based solely on a purely structural or aerodynamic focus. To quantify the interactions between the vehicle aerodynamics and structural design it was thus necessary to conduct an aero-structural optimization. This study utilized aero-structural trade factors determined by aerodynamic performance estimates to quantify system-level impacts of changes to wing and strut properties. A global FEM was used to establish a set of structural design requirements. These requirements were then used as constraints for an aerodynamic optimization performed using TRANAIR (2) with wing and strut box sizing in the loop. The resulting data were then used to inform a variety of vehicle design challenges.

An example of aero-structural optimization undertaken on the project was the examination of the strut/jury-strut relationship. One of the strut's most critical loading scenarios is when it is loaded in compression, as would be experienced in a negative-g pushover. In this case the strut's primary structural limitation is failure via column buckling. Assuming the strut is pinned at both ends, the key geometric design parameters are the length of the inboard and outboard strut segments (as determined by jury strut location), and the strut's transverse area moment of inertia distribution along its span – in this case the latter primarily being a function of strut airfoil shape and thickness. Since the aerodynamic interference in the wing-strut juncture region is particularly sensitive to airfoil shaping at transonic conditions, it was necessary to perform trades between airfoil thickness, strut length, and aerodynamic drag while minimizing weight. Results of the aero-structural optimization (depicted in Figure 5) suggested that an outboard movement of the jury strut from the location used in Phase III provided the best system-level performance.

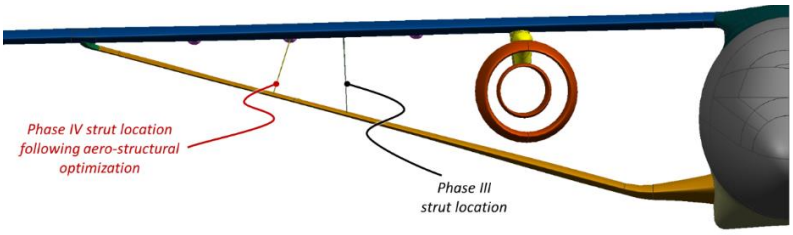

Figure 5. Jury Strut Optimization

By moving the jury strut outboard, the length of the strut element outboard of the jury was reduced. Since the maximum allowable buckling load is inversely proportional to the column length^2, this significantly reduced its strength requirements. This in turn enabled the outboard strut design to mitigate undesirable transonic interference drag in the wing-strut intersection by maintaining a locally low thickness. Since the strut region inboard of the jury strut attachment was aerodynamically less sensitive to an increase in strut thickness and chord, it was preferable at the system level to accept increased inboard strut strength requirements. Modifications to the inboard strut planform including increased chord and thickness were therefore undertaken to increase inboard strut strength. These modifications consequently further enabled the efficient generation of additional lift on the inboard strut. This philosophy was further reinforced by subsequent aerodynamic design optimization.

Aerodynamic performance estimates for the final configuration obtained using the NASA Reynolds-Average Navier-Stokes (RANS) Computational Fluid Dynamics (CFD) code OVERFLOW (3) (Figure 6) show that the TTBW vehicle is well-suited for operation at the design cruise Mach=0.80, with trimmed values for vehicle Lift-to-Drag ratio, L/D≈23. This compares well to the result obtained in Phase III, for which trimmed L/D values are only slightly higher despite the lower cruise Mach number.

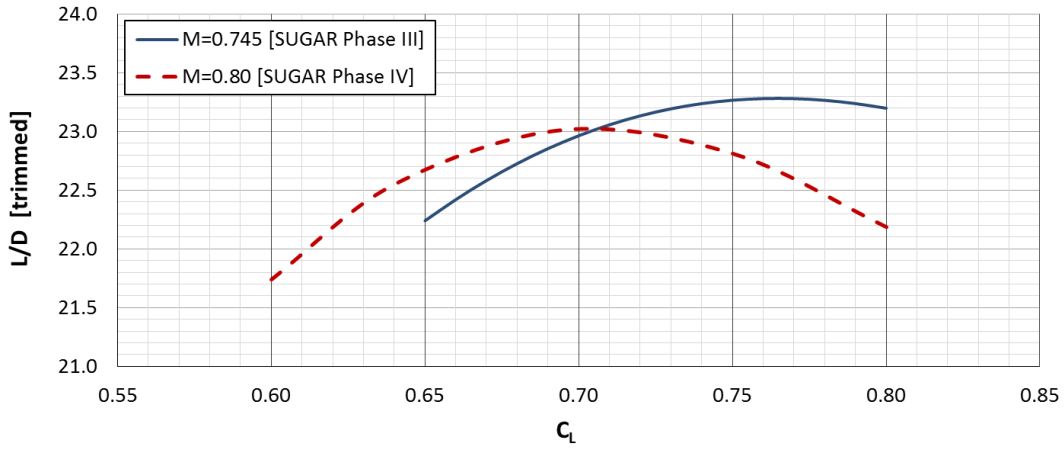

Figure 6. Final Vehicle L/D Performance [OVERFLOW – Flight Re, turbulent, trimmed]

When including the effects of cruise Mach number, the Phase IV design shows an improved aerodynamic efficiency as compared to the Phase III design. However, it should be noted that while the Phase III design utilized divergent trailing-edge airfoil technology not used in the Phase IV design, the configuration discoveries made in Phase IV regarding the strut planform offset effects and updated optimization methods could be retroactively applied to the Phase III design. This modification would potentially improve M=0.745 vehicle performance relative to the Phase IV design.

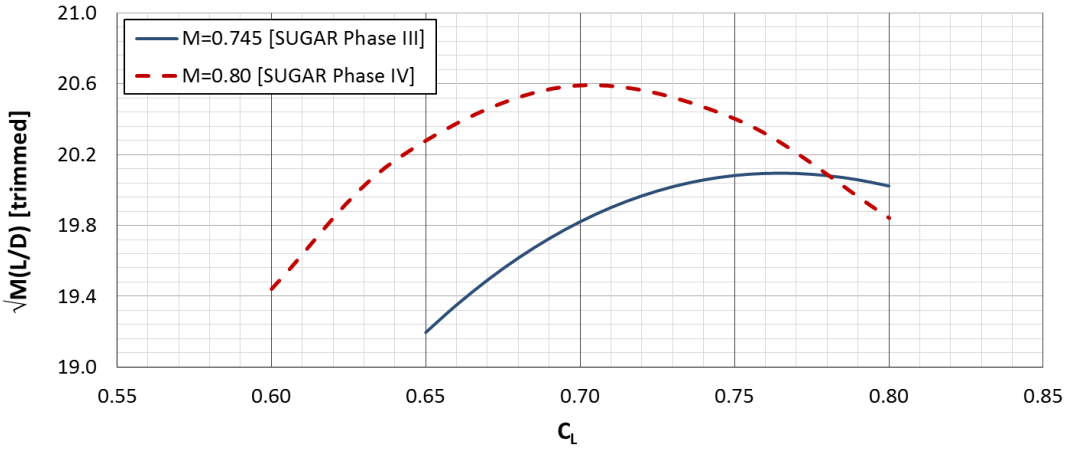

Figure 7. Final Vehicle $M^{1/2}$(L/D) Performance [OVERFLOW – Flight Re, turbulent, trimmed]

C. High-Speed Testing and Validation

Following the completion of the detailed high-speed aerodynamic design effort, the vehicle's aerodynamic performance was validated in a wind tunnel test in the 11-Foot Transonic Wind Tunnel (TWT) at the NASA ARC UPWT located at Moffett Field, CA beginning in July 2019. The M=0.80 model (shown in Figure 8) was built to the same 4.5% scale as the Phase III M=0.745 wind tunnel model. This enabled the re-use of many of the same model components, including the model strongback, fuselage, and empennage. More importantly, this enabled the test to begin with a repeat of the previous model geometry to ensure test-to-test repeatability of the aerodynamic performance and data processing routines.

Figure 8. M=0.80 TTBW Configuration in the NASA Ames 11-Foot TWT

Following a checkout of the Phase III geometry, the M=0.80 Phase IV geometry was installed. The primary objectives of the M=0.80 high-speed test were to:

1) Validate vehicle lift and drag performance
2) Assess longitudinal and lateral-directional stability characteristics
3) Conduct a preliminary assessment of vehicle flight controls effectiveness

The test evaluated the transonic performance of the vehicle across a range of conditions, capturing forces and moments and surface pressure data for all configurations. Compressibility effects were quantified through the collection of drag rise data. In addition, model aeroelastic deflection data was captured by the tunnel's Model Deformation Measurement (MDM) system for the 'complete' configuration (wing, strut, nacelle and pylon, empennage, and flap hinge fairings installed).

As distinct from the previous transonic testing, the M=0.80 model was not designed for a component-by-component build-up in the tunnel. In particular, the model was not designed for strut-off testing since this places considerable structural limitations on the wind tunnel model design. Specifically, strut-off wing strength requirements severely limit the amount of surface pressure instrumentation that can be placed in the model, while also limiting attainable Reynolds numbers. Therefore, the decision was made to exclude strut-off testing from the test plan. However, even though the resulting wing strength requirements were improved the model's small physical scale necessitated that the pressure rows on the wing and strut be divided between the left and right-hand surfaces. The spanwise location of the pressure instrumentation is depicted in Figure 9, represented by the red lines.

Figure 9. 4.5% Scale M=0.80 Transonic Wind Tunnel Model Deflectable Surfaces and Instrumentation

The location of the model's deflectable control surfaces are also shown in Figure 9, including inboard and outboard ailerons, spoiler panels, and horizontal stabilizer. During the test, these surfaces were deflected to a range of angles to determine their effectiveness.

As of December 2019, detailed analysis of the test results are in progress. However, a preliminary assessment of the data shows excellent repeatability of the M=0.745 configuration as compared to data from the previous transonic test entry, with drag results from the two tests repeating within the accuracy of the balance. Results for the M=0.80 configuration are also comparing well to pre-test CFD predictions. As shown in Figure 10, at the design lift coefficient (C_L=0.695) and dynamic pressure for which the model jig shape was computed (to account for aeroelastics) the tunnel-measured drag coefficient and CFD predictions agree within ~2 counts.

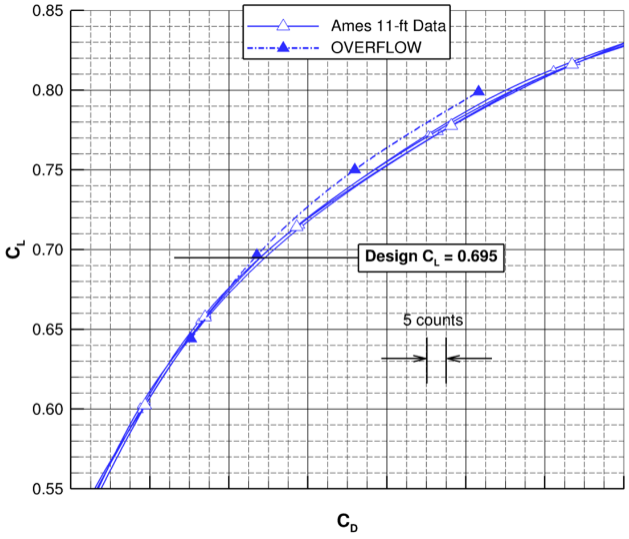

Figure 10. Transonic Performance Data from NASA ARC 11-Foot TWT Test [M=0.80, Re=5.25M/ft.]

D. Low-Speed Design

In Phase IV, development of the TTBW low-speed aerodynamic design continued, building on preliminary high-lift studies performed in Phase III. The high-lift system design task examined a variety of different system architectures to determine which approach could best enable the vehicle to meet its low-speed performance targets.

The study began with 2D investigations of the high-lift system by comparing the relative performance of different leading-edge concepts using the automated Boeing RANS CFD package ANTS (Automated Navier-Stokes Two-dimensional Setup). This package can vary device rigging parameters including gap, overhang, and deflection angle.

To maintain wing laminar flow compatibility, a leading-edge Krueger was assumed to be the baseline leading-edge device since a Krueger can protect the leading edge from contamination (bugs, ice, erosion, etc.) during low-speed operations. The preliminary design utilized a Fixed-Camber Krueger (FCK) variation. However, conventional slat, Variable-Camber Krueger (VCK), drooped leading edge, and morphing leading edge devices were also considered. The fixed-camber and variable-camber Krueger devices were sized based on scaling existing designs to estimate the volume required for the stowed actuation mechanism within the available space forward of the front spar. A detailed study to develop the actuation mechanism and kinematics was not included within the scope of the project. For the conventional slat, drooped leading edge, and morphing leading-edge devices, various device-to-wing chord ratios were evaluated. For the leading-edge design study, a starting baseline geometry was first developed for each device and then the key geometric parameters were systematically varied to provide a final optimized 2D design. All leading-edge device trade studies utilized a fixed wing trailing-edge geometry.

The results of the 2D study indicated that the variable camber Krueger architecture was preferred since it offered the best combination of performance and laminar flow compatibility. With the leading-edge device chosen, the trailing-edge flap shape and rigging positions were then analyzed for a range of takeoff and landing positions. These studies, which utilized a single-segment flap as a baseline geometry, focused on maximizing the takeoff L/D and landing C_{Lmax} as the primary design objectives. Each time the particular device geometric parameters were varied the rigged position was re-optimized using the ANTS tool and the results plotted using a MATLAB-based post-processing script. An example of the leading-edge and trailing-edge rigging optimization generated using the automated process is shown in Figure 11. These plots show contours of sectional maximum lift coefficient as a function of device rigging.

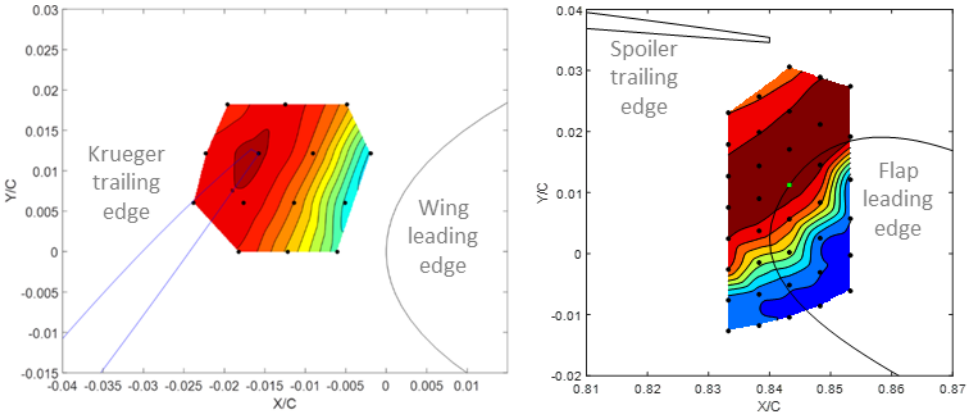

Figure 11. Example $c_{l_{max}}$ thumbprint rigging optimization contour plot for the leading edge (left) and trailing edge (right)

Once the 2D comparison of the leading edge concepts was complete, the preferred high-lift system architecture was adapted to the full 3D vehicle configuration. However, before the 3D high-lift system could be defined, the vehicle control surface architecture had to be determined. A study was therefore required to inform the layout of the high-lift system while ensuring that the vehicle had adequate control authority. To this end, five different control surface architectures were considered prior to the 3D high-lift system definition. Each of the five arrangements was evaluated for roll authority against requirements consisting of maximum steady state roll rate and time-to-bank for a range of cruise, maximum operating Mach, dive speed, and approach conditions. The candidate (and selected) high lift and control surface planform layouts are illustrated in Figure 12.

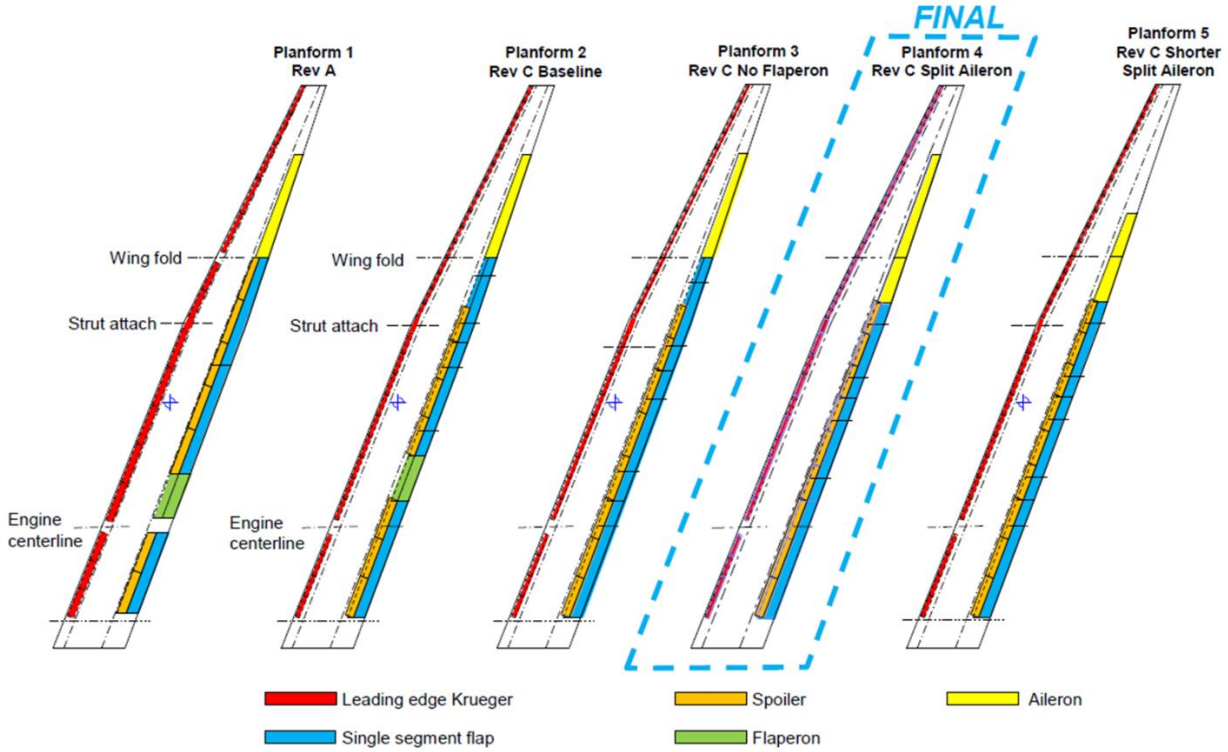

Figure 12. Candidate control surface architectures and final planform selection.

The study revealed that planform arrangements 2, 3, and 5 were inadequate in terms of meeting the time-to-bank requirement in the approach phase of the flight envelope. Planform arrangements 1 and 4 were found to have similar performance to each other in both the time-to-bank and steady roll rate requirements. However, planform 4 was expected to have better performance in terms of the high-lift system due to the continuous spanwise flap layout. As a result, planform 4 was selected as the preferred control system arrangement.

Once a control surface planform layout was selected, the results from the 2D leading-edge device study and single-segment flap optimization were used to develop the initial 3D loft and rigging of the TTBW high-lift system. CFD analysis in OVERFLOW was employed to investigate the system's high-lift performance, and to refine the rigging of both the leading-edge Krueger and the trailing-edge flap in a fully 3D flowfield. The results of the 3D studies indicated that the initial rigging determined by 2D analysis provided insufficient protection of the outboard wing and would thereby require significantly different Krueger deflections than what had been predicted. To mitigate this concern, the final 3D-optimized configuration divided the outboard wing Krueger (the portion from the wing leading-edge break out to the wingtip) into five spanwise segments. These outboard Krueger segments required a significant differential deflection angle from the inner-most segment to the outer-most segment in order to maintain acceptable stall behavior. However, due to the challenges of using RANS-based CFD tools for accurate high-lift predictions, the final rigging of the leading-edge device was determined during low-speed wind tunnel testing.

In addition to the high-lift system design, the effects of the strut on the vehicle's low-speed aerodynamic performance was assessed. Since there were no pre-existing configurations with a similar layout, the effects of the strut on the vehicle's stall behavior and wing high-lift system were unknown. As similar to the other high-lift analysis tasks, this study relied on results obtained from 3D analysis in OVERFLOW. The results indicated that at flight Reynolds number the strut did not experience a significant degree of flow separation, with the vehicles' primary stall mechanism driven by the wing. The addition of the strut to the configuration resulted in an increase in the lift curve slope primarily due to the change in loading across the span of the strut as the angle of attack is increased. As previously noted, it is likely that the inboard strut's aft location and proximity to the wing (and body) were protecting it from significant variation in local angle of attack, while the outboard strut flow behavior is primarily determined by the flowfield generated from the wing. The strut did not appear to require leading edge high-lift treatment for low-speed operations. The study also showed that while the presence of the strut had a minimal influence on the portion of the wing outboard of the strut attach location, the effects of the strut's presence on the inboard wing and Krueger were significant enough to require the inclusion of the strut during the 3D Krueger and flap rigging optimization.

In addition, although computational results did not show that the stall initiation in the landing configuration was driven by the presence of the nacelle/pylon, nacelle strakes were evaluated in different axial and radial locations using CFD on the inboard side of the nacelle to determine any potential benefit to vehicle performance. Computational results confirmed that the strakes were relatively ineffective on this configuration. However, a final strake position optimization was planned for the low-speed wind tunnel testing.

E. Low-Speed Testing and Validation

Following the completion of the detailed high-lift aerodynamic design effort, the vehicle's low-speed aerodynamic performance was validated in a wind tunnel test in the NASA LaRC 14- by 22-Foot Subsonic Tunnel located in Hampton, VA beginning in September 2019. The primary objectives of this test were:

1) Develop a high-lift performance database, including: component build-up, leading- and trailing-edge rigging studies, nacelle strake optimization, strut flap performance, and landing gear increments
2) Develop a stability and control database, including vehicle lateral-directional properties, control surface effectiveness, and trim effects

The low-speed model (shown in Figure 13) is an 8.0% scale representation of the TTBW vision vehicle. The model's oblique ventral sting support – in which the model support penetrates the lower, aft fuselage – was selected since it minimized interference of the sting with the wing, strut, and empennage. The model was designed with the flexibility such that the support sting could alternately be mounted in a dorsal position. In the dorsal position the model empennage is removed and the sting penetrates the model on the aft upper fuselage (a near mirror of the ventral position). This capability was designed into the model in anticipation of potential future testing needs; the dorsal mount enabled the model to be either inverted for potential acoustic testing, (the 14- by 22-Foot Tunnel's acoustic array is mounted on the ceiling), or to be tested in ground effect.

Figure 13. TTBW Low-Speed Test in the NASA LaRC 14- by 22-Foot Subsonic Tunnel

The locations of the low-speed model's deflectable control surfaces, including inboard and outboard ailerons, inboard, mid, and outboard spoiler banks, horizontal stabilizer, elevator, and rudder are shown in Figure 14. During the test, these surfaces were deflected to a range of angles to determine their effectiveness. The model flaps and leading-edge Kruegers could be tested at a range of deflection angles, and their gap and overhang position could be varied using a series of brackets, shims and spacers. In addition, the spoilers could be drooped to allow designers to investigate the potential for additional high-lift performance. The model also had removable landing gear, and a simple strut flap.

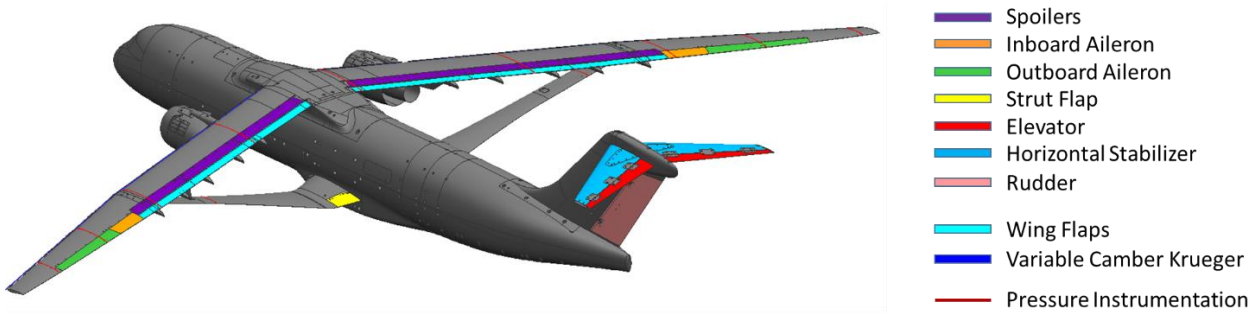

Figure 14. 8.0% Scale M=0.80 High-Lift Wind Tunnel Model Deflectable Surfaces and Instrumentation

The test evaluated the low-speed performance of the vehicle across a range of conditions, capturing forces, moments, and surface pressure data for all configurations. The locations of surface pressure instrumentation are shown in Figure 14 with red lines.

As of December 2019, post-test data analysis of the results is in progress. Therefore, only a preliminary set of conclusions is available at this time. In general, the performance of the high-lift system met expectations. The leading-edge variable camber Krueger and the trailing-edge flaps in the landing configuration produced stall angles and maximum lift levels consistent with computational predictions. However, to obtain the desired performance and vehicle stall character the optimized Krueger rigging determined by CFD required in-tunnel refinement, particularly on the outboard wing panel. Lift curves and drag polars for the cruise, Krueger extended, takeoff, and landing configurations are shown in Figure 15.

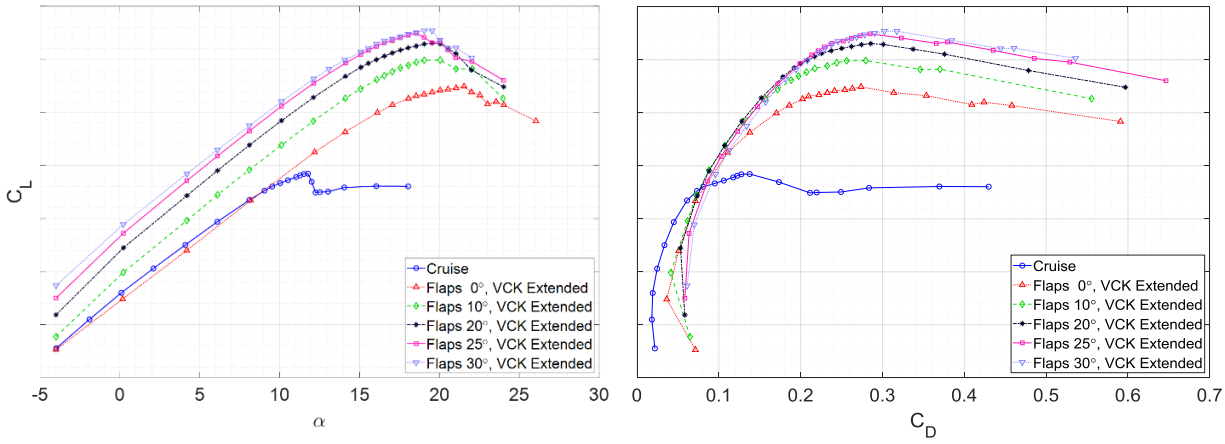

Figure 15. Selected Low Speed Wind Tunnel Test Results [M=0.2, Re=1.4M/ft]

F. Structural Design and Aeroelastic Analysis

In addition to the aerodynamic development work undertaken in this phase of the contract, the concept's structural design was also addressed. This work comprised the development of key joint concepts, and the development of a finite element model (FEM) to be used for airframe structural sizing and weight estimation. This FEM was then used for a more detailed assessment of the vehicle's aeroelastic behavior and performance.

1. Conceptual Fitting/Attachment Design

Several concepts were investigated for key structural connections at the strut-body and wing-strut interfaces. A fail-safe swivel joint at the inboard end of the main strut (where the strut connects to the body) was developed to limit the strut structure to axial loading only. If practical, this concept would significantly simplify the design and construction of the strut structure. For the wing-strut connection, a curved fitting was designed to offset the strut from the wing lower surface in order to reduce aerodynamic coupling between these surfaces. The increased weight of the curved offset joint is expected to be offset by reduced aerodynamic interaction, as well as manufacturing benefits from reduced local curvature of the wing lower surface in the wing-strut channel.

While these concepts are not currently part of the baseline structural concept for the vehicle, the results of these studies suggest that there are still potential benefits for pursuing their development as a part of a future design effort. As application of these concepts may affect internal loads, the next step in development would be to represent them in the vehicle FEM and analyze them in higher detail.

2. Global FEM Refinement and Aeroelastic Analysis

When moving to the SUGAR Phase IV TTBW geometry, modifications to the configuration were significant enough to require a re-examination of the vehicle structural design. In particular, it was important to verify that these changes did not have a significant negative effect on the vehicle weight or aeroelastic stability. To this end, a detailed FEM of the Mach 0.80 configuration, shown in Figure 16, was developed. This refined model was sized for typical maneuver and gust load design conditions, and flutter analyses were performed. The aeroelastic loads analyses used theoretical doublet lattice (DL) aerodynamics, while the subsequent flutter analysis used correction factors to match CFD results.

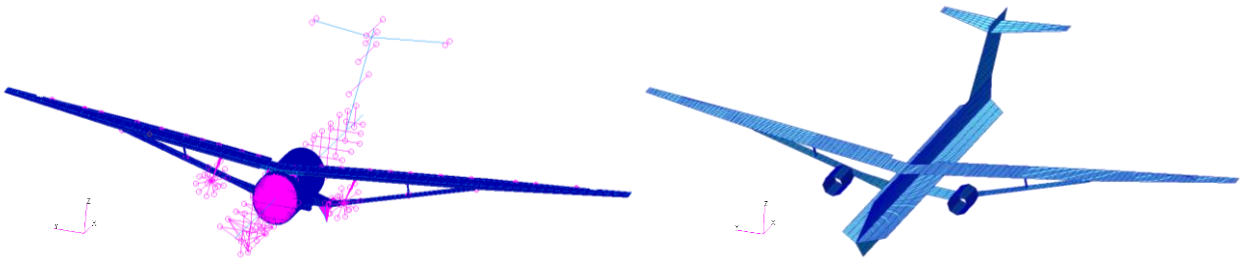

Figure 16. Updated Integrated Vehicle Finite Element Model (left) and Doublet Lattice Aerodynamic Model with Refined Mesh (right)

Aeroelastic Loads and Sizing

Maneuver loads consisting of 2.5g pull ups, -1g push overs, and 1g steady flight were analyzed at multiple flight conditions and mass cases. Gust loading was evaluated at critical conditions to capture the maximum vehicle response over the design flight envelope through tuned discrete gust analysis. Internal loads results showed the large effect of the strut in reducing wing shear and bending loads. A critical loads selection process identified nine gust conditions and two maneuver conditions for use in structural sizing. While maneuver loads were higher over portions of the outer wing, gust loads were dominant over most of the inboard wing.

The wing, strut, and jury structures were optimized to minimize weight and meet strength and buckling constraints. The total wing weight (for the sized structure) was within 100 pounds of the weights from the earlier M=0.745 analysis during Phase II and Phase III. Additional optimization runs with different parameters produced similar results. These results gave confidence that the M=0.80 configuration has no major issues for achieving a weight that meets requirements.

Flutter Analysis

The high aspect ratio of the TTBW wing results in low structural mode frequencies, and bending modes in both the normal and in-plane directions. Several of these modes are close in frequency, with potential to coalesce under unsteady aerodynamic loading. The initial flutter analysis without CFD adjustments, using raw DL aerodynamics, predicted adequate stability margins at all flight conditions, with the lowest margin at the Mach 0.92 design dive speed. To improve flutter analysis fidelity, aerodynamic adjustments based on CFD analyses were developed and applied to the unsteady aerodynamic wing loads predicted by the DL method. For the CFD-based analysis results, healthy airspeed margins were predicted at flight conditions up through Mach 0.85. However, at Mach 0.92 the results were inconclusive. A flutter analysis with the unsteady aerodynamic modal loads predicted with CFD directly is required for this condition, and is a topic for future work.

Additional aeroelastic analysis tasks remain to be addressed in the future. Because the TTBW configuration results in a redundant wing load path unlike that of a cantilevered wing, flutter analysis should be performed with pre-stressed modes and potentially about a large deformation operating state. This has been investigated in the past, and should be revisited for the current TTBW configuration. In addition, maneuver and gust load analyses should be updated with CFD-based aerodynamic adjustments as was done for flutter analyses.

In summary, available aeroelastic analyses to date suggest the TTBW aircraft configuration is feasible. Structural sizing optimization using critical maneuver and gust loads yielded reasonable wing and strut weights in line with the predictions of previous TTBW development work. Aeroelastic stability analyses incorporating CFD-based aerodynamic adjustments suggest healthy flutter margins at Mach numbers up through 0.85. Higher fidelity analyses are required at higher Mach.

IV. Conclusion

A TTBW concept has been developed for a design cruise Mach number of 0.80. Detailed high-speed aerodynamic design shows that the TTBW concept is well suited for operation at this condition. High aerodynamic efficiency predictions at cruise have been validated in a high-fidelity wind tunnel test in the NASA ARC 11-Foot TWT. High-lift system design of the TTBW has yielded low-speed performance in-line with expectations. Results from computational studies and wind tunnel testing in the NASA LaRC 14- by 22-Foot Subsonic Tunnel have demonstrated the necessity of differential Krueger rigging on the outboard wing panel. However, there remains significant potential for high-lift system performance improvement with additional study. Structures development also continued under Phase IV, with revisions to the vehicle FEM and a high-fidelity aeroelastic analysis performed. Results from this analysis highlight the necessity of higher-fidelity flutter analysis going forward. Although aeroelastic analysis performed to date supports the conclusion that the TTBW concept is feasible, work still remains to resolve aeroelastic stability questions at dive speeds.

V. Future Areas of Study

The work undertaken in SUGAR Phase IV has continued to systematically address the highest risk items regarding the suitability of the TTBW concept as a commercial transport. In this phase researchers sought to address whether the TTBW concept can be designed to operate efficiently at Mach numbers consistent with today's commercial aircraft fleet. Based on the results of this study, there is sufficient data to support continued research of the TTBW concept. To further mature the concept and reduce risk, there are several identifiable areas where continued focus would be best concentrated. These areas include (in no specific order):

1) Buffet: Conduct a detailed investigation of the aerodynamics of high-speed buffet, with concentration on wing-strut-channel and low-C_L induced buffet.
2) High-Lift System Design: Continue detailed studies of alternate high-lift system architectures, and perform system-level trades.
3) High-Lift System Validation: Acquire in-ground-effect data. Perform a high-Reynolds number wind tunnel test of the high-lift system.
4) High-Re Transonic Performance Validation: Conduct a high Reynolds number transonic wind tunnel test of the cruise configuration.
5) Aeroelastic Analysis: Continue detailed aeroelastic stability analysis. Increase fidelity of current modeling to include elasticity in key structural joins.
6) Detailed Structural Design: Develop a complete, fully integrated vehicle structural design, and develop a roadmap for demonstration of key structural concepts.
7) Aero-Structural Optimization: Conduct detailed multi-disciplinary optimization studies to focus on significant variations in vehicle architecture, such as alternate wing-strut tie-in locations.
8) Acoustic Assessment: Assess the acoustic performance of the configuration and validate in a wind tunnel test. Develop a roadmap for demonstration of key acoustic technologies.
9) Certification Challenges: Investigate unique TTBW certification challenges including: damage tolerance (birdstrike, crashworthiness), ditching characteristics, and icing effects (accretion, aerodynamic effects, and protection).

Acknowledgments

The results presented in this paper reflect the combined efforts of the Boeing enterprise SUGAR team. The authors would like to recognize Anthony Sclafani for aerodynamic design support and CFD analysis, Lie-Mine Gea and Mark Dehaan for CFD analysis, David Lazzara for Aero and Aero-structural Optimization, Gary Ige, Peter Wilcox, Mike Ferris, David Pitera, Leo Chou, Khanh Pham, Bruce Detert, Paul Vijgen, Steve Chapel, Jonathan Vass, and Elmer Tse for wind tunnel test support, Peter Camacho and David Bruns for aerodynamic performance analysis, Niko Intravartolo and Jeffrey Jonokuchi for stability and control analysis, Paul Miller for weights analysis, Ryan Michel and Robert Creason for structures design and analysis, and Eric Reichenbach for leading the aeroelastic analysis.

Funding for this effort was provided by the NASA Fundamental Aeronautics Program, through the Subsonic Fixed Wing Project followed by the Advanced Air Vehicles Program, through the Advanced Air Transport Technology Project. The contract number is NNL16AA04B task order NNL17AA46T.

References

1. **NASA.** *Strategic Implementation Plan.*
2. —. TRANAIR. [Online] https://ntrs.nasa.gov/archive/nasa/casi.ntrs.nasa.gov/19950021809.pdf.
3. **Nichols, R. and Buning, P.** *User's Manual for OVERFLOW Version 2.1t.* 2008.
4. **Bradley, M. and Droney, C.** *Subsonic Ultra Green Aircraft Research: Phase I Final Report.* s.l. : NASA CR-2011-216847, 2011.
5. **Bradley, M., Droney, C., and Allen, T.** *Subsonic Ultra Green Aircraft Research Phase II: Volume I - Truss Braced Wing Design Exploration.* s.l. : NASA CR-2015-218704/VOL1, 2014.
6. **Allen, T., Bradley, M., and Droney, C.** *Subsonic Ultra Green Aircraft Research Phase II: Volume III - Truss Braced Wing Aeroelastic Test Report.* s.l. : NASA CR-2015-218704, 2014.
7. **Bradley, M., and Droney, C.** *Subsonic Ultra Green Aircraft Research Phase II: Volume II - Hybrid Electric Design Exploration.* s.l. : NASA CR-2015-218704/VOL2, 2014.
8. *Subsonic Ultra-Green Aircraft Research: Transonic Truss-Braced Wing Technical Maturation.* **Droney, C., Harrison, N., and Gatlin, G.** Belo Horizonte, Brazil : s.n., 2018. 31st Congress of the International Council of the Aeronautical Sciences (ICAS).
9. **Droney, C., Sclafani, A., and Grasch, A.** *Subsonic Ultra-Green Aircraft Research Phase III: Mach 0.745 Aerodynamic Design.* s.l. : NASA CR-2018-xxxx, 2015.